Optimized transfers between Quart-monde invariant manifolds

Laurent Beauregard, Emmanuel Blazquez, Stéphanie Lizy-Destrez

OPTIMIZED TRANSFERS BETWEEN EARTH-MOON INVARIANT MANIFOLDS

Laurent Beauregard, Emmanuel Blazquez, Stéphanie Lizy-Destrez

ISAE-SUPAERO, 10 Avenue Edouard Belin, 31400 Toulouse

ABSTRACT

The future habitable space station, the Lunar Orbital Platform-Gateway (LOP-G), will, most likely, be placed in a southern L_2 Near Rectilinear Halo orbit. A significant body of work remains to be done on the design of the rendezvous procedure between Halo orbits. Given a fixed start and end Halo orbits, direct transfers between the two can produce simple strategies with short transfer time at the cost of relatively high velocity increment Δv. When longer transfer time is allowed, as with some cargo, lower energy transfers, taking advantage the natural dynamics of the Earth-Moon system, can be used. Commonly used topological structure are the stable and unstable manifold of a given orbit. These trajectories can be used to transfer a spacecraft from one Halo orbit to another Halo orbit at a low cost. In this article, several transfer methods will be compared.

Index Terms— Optimization, Earth-Moon system, NRHO, Transfer, Manifolds

1. INTRODUCTION

As a successor of the International Space Station, the Lunar Orbital Platform-Gateway (LOP-G) will be a space station placed in cis-lunar space. Its will act as a scientific hub and will allow easy access to the lunar surface. The position of the LOP-G is tentatively chosen to be a L_2 southern Near Rectilinear Halo Orbit (NRHO) of the Earth-Moon system of period 6.56 days and an apoapsis altitude of 1500 km above the surface of the Moon [1]. A significant amount of research is being done on the transfer to and from Halo orbits. One procedure involves going to an intermediate Halo orbit as part of the far approach maneuver. There is still an open question as to the best method to transfer from one Halo orbit to the other. In this article, three transfer methods will be discussed and compared for lowest total change in velocity Δv. The first method is a quasi-static approach, used as a benchmark to provide an upper bound on the Δv requirement. The next method will consider optimized Lambert arcs. The last method will use the stable and unstable manifold of the orbits and their intersections. While invariant manifolds have been used before for transfers [2][3][4], this article will describe a procedure to obtain a one dimensional set of intersection between the manifolds along with a Δv optimization procedure over these intersections.

2. CIRCULAR RESTRICTED THREE BODY PROBLEM

In the vicinity of the Earth-Moon system, it can be approximated, as a first order, that the only gravitational contributions come from the Earth and the Moon [5]. If the Moon is further assumed to move in a circular orbit, this is called the circular restricted three body problem (CR3PB). The orbital plane of the Moon is the x-y plane and the period of revolution is

$$T = 2\pi\sqrt{\frac{a^3}{\mu_E + \mu_M}} \sim 27.28 \text{ days} \tag{1}$$

Where μ_E and μ_M are the standard gravitational parameter of the Earth and the Moon respectively and a is the distance between the Earth and the Moon. The origin of the frame is chosen to be the barycenter of the Earth-Moon system $\hat{\imath}, \hat{\jmath}, \hat{k}$ are units vectors in the x, y, z direction respectively. The frame is oriented such that the Earth and Moon lies on the x-axis with the Earth in the direction of -x and the Moon +x. The z-axis is defined by the direction of the rotation of the Moon $\vec{\omega}$. Its expression is given by

$$\vec{\omega} = \sqrt{\frac{\mu_E + \mu_M}{a^3}}\hat{k} \tag{2}$$

It is straightforward to show that the position of the Earth $\vec{r}_E$ and the position of the Moon $\vec{r}_M$ are

$$\vec{r}_E = -\frac{\mu_M}{\mu_E + \mu_M}\hat{\imath} \ , \ \vec{r}_M = \frac{\mu_E}{\mu_E + \mu_M}\hat{\imath} \tag{3}$$

The acceleration of a third massless body in this rotating frame is given by

$$\begin{aligned}\ddot{\vec{r}} = &-\frac{\mu_E}{|\vec{r} - \vec{r}_E|^3}(\vec{r} - \vec{r}_E) - \frac{\mu_M}{|\vec{r} - \vec{r}_M|^3}(\vec{r} - \vec{r}_M) \\ &- \vec{\omega} \times (\vec{\omega} \times \vec{r}) - 2\,\vec{\omega} \times \dot{\vec{r}}\end{aligned} \tag{4}$$

where $\vec{r}$, $\dot{\vec{r}}$ and $\ddot{\vec{r}}$ are the vectorial position, velocity and acceleration of the massless body. The reduction to first order ODE can be done

$$\frac{d}{dt}\begin{pmatrix}\vec{r} \\ \vec{v}\end{pmatrix} = \begin{pmatrix}F_r \\ F_v\end{pmatrix} \tag{5}$$

with $F_r = \vec{v}$ and F_v the right-hand side of equation 4 with $\dot{\vec{r}} = \vec{v}$. The evolution of the state transition matrix is given by the matrix differential equation

$$\frac{d}{dt}\begin{pmatrix} M_{rr} & M_{rv} \\ M_{vr} & M_{vv} \end{pmatrix} = \begin{pmatrix} \partial_r F_r & \partial_v F_r \\ \partial_r F_v & \partial_v F_v \end{pmatrix}\begin{pmatrix} M_{rr} & M_{rv} \\ M_{vr} & M_{vv} \end{pmatrix} \quad (6)$$

The data for the various orbital parameters are given in table 1 [6]. The dynamical system, eq. 4, can be shown to have 5 fixed point, the Lagrange points. Three are co-linear L_1, L_2, L_3 and two are triangular L_4, L_5 [7].

Table 1. Orbital data

$\mu_E\ (km^3/s^2)$	398600.4415
$\mu_M\ (km^3/s^2)$	4902.8005821478
$a\ (km)$	384400

This dynamical system is often adimensionalized by choosing units for which $\mu_E + \mu_M = 1$ and $a = 1$. This implies the scale in table 2

Table 2. Adimensionalized unit conversion factor

Time scale (s)	375190.259
Length scale (km)	384400
Velocity scale (km/s)	1.02454685531

3. HALO ORBIT THEORY

Halo orbits start to exist as a bifurcation of the planar Lyapunov orbits associated with L_1 or L_2. Several parametrizations of Halos exist, a common one originates from applying the Poincaré–Lindstedt method to obtain an approximation of the Halo orbit and then specifying the amplitude "A_z" of the out-of-plane component and lastly applying a refinement procedure to obtain a closed orbit [7]. This parametrization suffers the drawback of being a one-way function, that is, given the points of the Halo orbit $(r(t), v(t))$, it is not trivial to retrieve the A_z that generated this orbit. In this article, the parametrization chosen is the out of plane component of the velocity V_z at the crossing of the x-y plane, i.e $z = 0$. This can be readily obtained from the state vector $(r(t), v(t))$ alone and is unique for every Halo orbit. It increases from 0 close to the planar Lyapunov to a maximum for NRHOs. Another valid parameter is the periapsis P_e distance to the Moon. Figure 1 and 2 provide the relation between the commonly used variables A_z, P_e and V_z.
Up to an A_z of 60000 km, there is an approximate linear relation between A_z and V_z described by eq. 7.

$$V_z = \frac{4\ m/s}{1000\ km} A_z \quad (7)$$

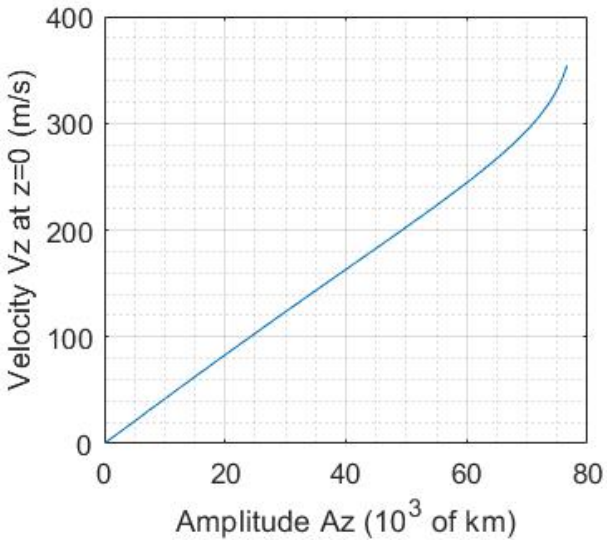

Fig. 1. Relation between the amplitude A_z and V_z

The relation between the periapsis distance P_e and V_z is approximated by equation 8 with P_e expressed in 10^3 km and V_z is m/s

$$V_z = \frac{1683}{\sqrt{Pe + 2.25}} \quad (8)$$

The stability of a closed trajectory can be determined from the eigenvalues of the differential of the Poincaré map [8]. The real and imaginary parts of these eigenvalues for L_2 orbits are shown in figure 3.
Four distinct sections of stability are identified

- Regular Halo orbit: V_z = 0 to 400 m/s
- Stable/Neutral Halo orbit: V_z = 400 to 450 m/s
- Regular NRHO: V_z = 450 to 1150 m/s
- Stable/Neutral NRHO: V_z = 1150 to 1200 m/s

4. QUASI-STATIC APPROACH

Two limiting cases for orbital transfers include instantaneous and infinitesimal propulsion, corresponding to the limit of infinite or zero thrust respectively. In the case of two body orbital dynamics, with central body having a standard gravitational parameter μ, the most efficient impulsive transfer between two circular co-planar orbits is a Hohmann transfer (except for some bi-elliptic transfers). The first and second impulse Δv_1 and Δv_2 to transfer from orbit of radius a_1 to

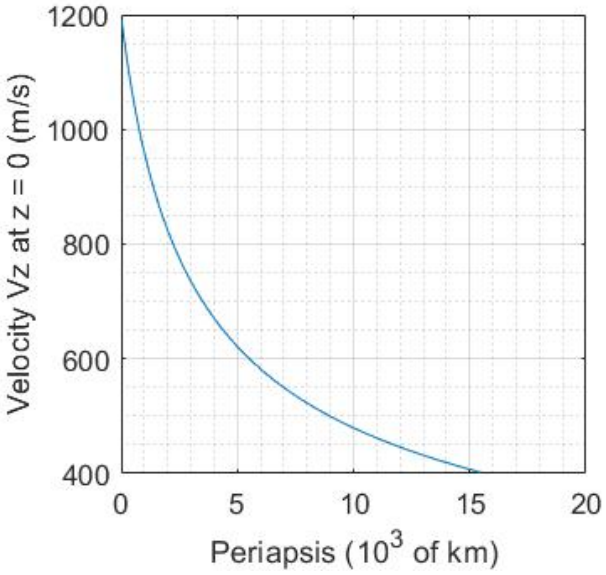

Fig. 2. Relation between the periapsis P_e and V_z

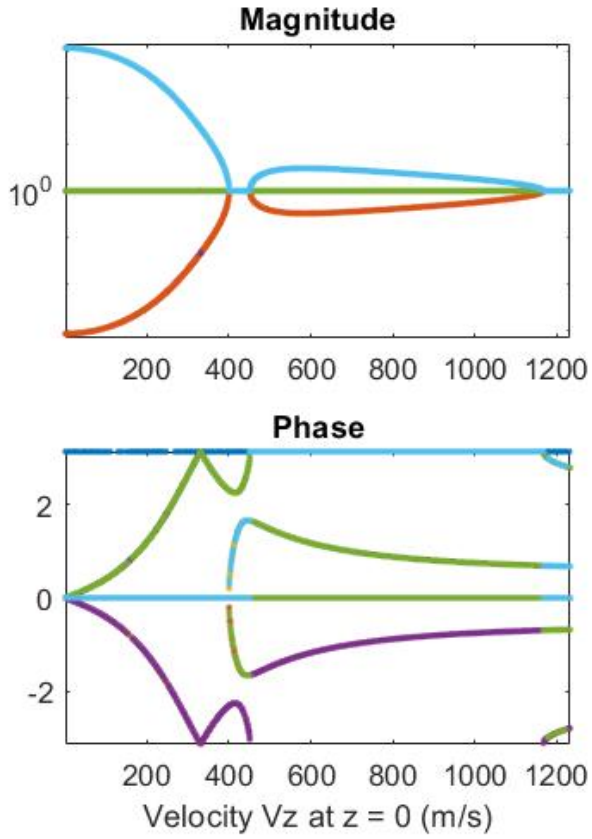

Fig. 3. Eigenvalues λ of the differential of the poincaré map for the family of L2 southern Halo

orbit with radius a_2 are given by equation 9 and 10

$$\Delta v_1 = \sqrt{2\mu\left(\frac{1}{a_1} - \frac{1}{a_1 + a_2}\right)} - \sqrt{\frac{\mu}{a_1}} \tag{9}$$

$$\Delta v_2 = \sqrt{\frac{\mu}{a_2}} - \sqrt{2\mu\left(\frac{1}{a_2} - \frac{1}{a_1 + a_2}\right)} \tag{10}$$

$$\Delta v_{\text{Hoh}} = \Delta v_1 + \Delta v_2 \tag{11}$$

The limit of an infinitesimally low thrust trajectory between the two same orbit can be shown to give a total Δv of

$$\Delta v_{\text{Low}} = \sqrt{\frac{\mu}{a_1}} - \sqrt{\frac{\mu}{a_2}} \tag{12}$$

Conceptually and numerically, a low thrust trajectory can be obtained by a large number of Hohmann transfers of increasing radius $a_1 \to \tilde{a}_1 \to \cdots \to \tilde{a}_N \to a_2$. Expanding the difference between a low thrust trajectory and the Hohmann transfer $\Delta v_{\text{Low}} - \Delta v_{\text{Hoh}}$ as a function of the altitude difference $a_2 - a_1$ results in a lowest non-zero term of order of three as shown in eq. 13.

$$\Delta v_{\text{Low}} - \Delta v_{\text{Hoh}} \sim \frac{1}{32}\sqrt{\frac{\mu}{a_1}}\frac{(a_2 - a_1)^3}{a_1^3} \tag{13}$$

One can conclude that for sufficiently close orbits, the cost of a low thrust trajectory can approximated (to the third order) to a Hohmann transfer and vice-versa. This result is the basis for the following analysis.

Given a finely spaced enough sampling of the L_2 family of Halo orbits, one can perform an analogous procedure and find transfers between all adjacent orbits. Similarly to the two body dynamics, this gives an upper bound on the transfer cost Δv between any Halo orbits, obviously at the cost of high flight time. One advantage of this approach is that at every intermediate stage of the transfer, the vehicle is in a closed orbit. The computation of the transfers is done as follow. Given two close Halo orbits, labeled A and B, and two points a and b on their respective Halo, there is always a natural candidate for the time of flight (ToF) to go from a to b: identify the point c on A that is closest, in space, to b. A first guess to the ToF is the amount of time it takes to travel from point a to c. One then applies a Newton's method with variable v_a, the initial velocity at a, to converge to b. This Newton's method is also allowed to change the time of flight. The geometry of this procedure is illustrated in figure 4.
Having three equations to solve (arriving at b) but four variables (v_a and ToF), there is still room for some optimization. While one would want to optimize the total $\Delta v = |\Delta v_a| + |\Delta v_b|$ with respect to the ToF, such an optimization is computationally expensive because the underlying equations are non-linear. The objective function to

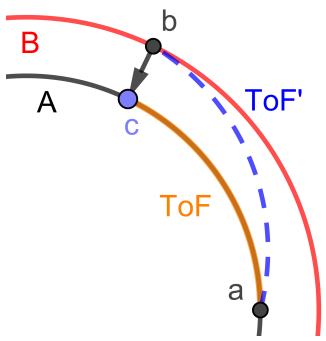

Fig. 4. Quasi-static transfer methodology between neighboring orbit

optimize is taken to be the sum of squares of Δv's i.e cost = $|\Delta v_a|^2 + |\Delta v_b|^2$. The cost can be written as

$$\min_{\Delta T} \Big[(\Delta v_a^0 + \Delta v_a)^2 + (v_a^* - v_b + M_{vv}\Delta v_a + F_v \Delta T)^2\Big] \tag{14}$$

With the following constraint

$$r_b = r_a^* + M_{rv}\Delta v_a + F_r \Delta T \tag{15}$$

where Δv_a^0 is the previous guess of the velocity increment, $r_a^* = r(ToF)$, $v_a^* = v(ToF)$ are the end point and velocity of the guessed trajectory, $M_{rv} = M_{rv}(ToF)$, $M_{vv} = M_{vv}(ToF)$, the components of the state transition matrix at the final state and $F_r = F_r(ToF)$, $F_v = F_v(ToF)$ the component of the dynamics at the final time. This problem has a unique solution

$$\Delta T = \frac{-X \cdot Y - Z \cdot W}{X^2 + Z^2} \tag{16}$$

$$\Delta v_a = M_{rv}^{-1}\left(r_b - r_a^* - F_r \Delta T\right) \tag{17}$$

Where

$$X = -M_{rv}^{-1} F_r \tag{18}$$

$$Y = \Delta v_a^0 + M_{rv}^{-1}\left(r_b - r_a^*\right) \tag{19}$$

$$Z = F_v - M_{vv} M_{rv}^{-1} F_r \tag{20}$$

$$W = v_a^* - v_b + M_{vv} M_{rv}^{-1}\left(r_b - r_a^*\right) \tag{21}$$

the update is $ToF \rightarrow ToF + \Delta T$ and $\Delta v_a^0 \rightarrow \Delta v_a^0 + \Delta v_a$. If this algorithm converges, the trajectory will have a locally minimum sum of squares of Δv's with respect to the time of flight. The next step is to divide each orbit in N points, either separated by fixed distance in space or by fixed orbital time. The above algorithm can then be used on every possible pairs. The computational burden may be reduced by limiting the maximum time of flight. Once that is complete, the lowest value Δv is kept. Further refinement can be done by varying the best points locally for a lower Δv, a pattern search is employed to this effect. This local optimization provides a lower cost Δv.

Figure 5 depicts the differential cost

$$\frac{d\Delta V}{dV_z} \tag{22}$$

of hopping between neighbouring orbit. Near the horizontal Halos, the cost is essentially 1 to 1. It increases and reaches a peak near V_z = 200 m/s, costing 1.5 m/s of Δv to increase V_z by 1 m/s. In the NRHO family, the cost to change orbit is small.

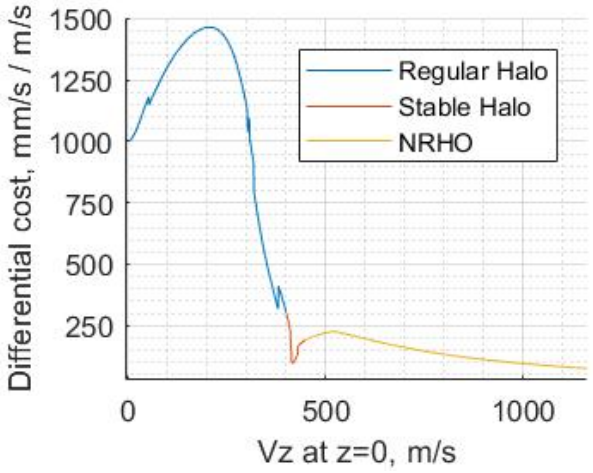

Fig. 5. Cost of hopping between neighbouring Halo orbits

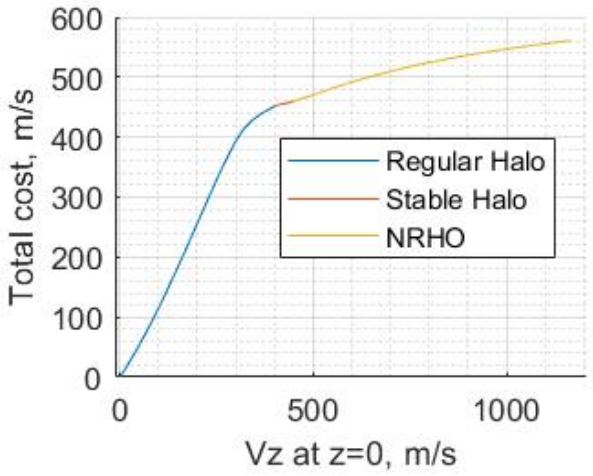

Fig. 6. Cumulative cost from Halo to Halo orbit using the Quasi-static approach

Figure 6 shows the cumulative cost from one Halo orbit to another. Interestingly enough, the whole L_2 Halo family can be covered with roughly 560 m/s. All NRHOs are covered with approximately 100 m/s. This hopping procedure was done both ways, from V_z: $0 \rightarrow 1200$ and $1200 \rightarrow 0$: the results are identical.

5. OPTIMIZED LAMBERT ARC

The Lambert problem for a dynamical system is: given two points in space r_1, r_2, a departure time t_1 and an arrival time t_2 find a (or all) trajectory $r(t)$ such that $r(t_1) = r_1$ and $r(t_2) = r_2$. Equivalently, one can solve for the initial velocity v_1 that produces the correct trajectory. For the two body problem, this problem is fully solved: given any two (non-colinear with the central body) points in space and a flight time T, there exist two unique trajectories which satisfy the Lambert problem [9]. In the case of the CR3PB, this problem has no simple solution. In fact, it is unclear how many solutions the problem has or if it even has solutions at all. Putting these issues aside, several methods can be employed to find solutions to Lambert's problem. A simple method is based on the fact that for sufficiently short flight time ToF, one possible trajectory can be approximated by a line connecting r_1 and r_2. In that case the velocity $v_1 = \frac{r_2 - r_1}{ToF}$. One must then use a Newton's method to correct v_1 to obtain $r(ToF) = r_2$. If ToF is sufficiently short (and there is no singularly in the line between r_2 and r_1), this method is guaranteed to converge for the CR3PB. Next, one increases the time of flight incrementally using the initial velocity v_1 from the previous iteration, performing a Newton's method at every step, until the desired time of flight is obtained. While this method always produces a solution, the trajectory obtained often have very costly out-of-plane maneuvers. Since the total Δv should be minimized, the algorithm described in chapter 4 can sometimes be used successfully even when orbits are not close. The further the orbits are, the less likely the algorithm is to converge and produce a connecting trajectory between two points on the Halos. By considering many departure and arrival points on the starting and final orbit, it is often possible to obtain a number of trajectories and so a Δv figure. An example of a set of trajectories are depicted in figure 7. Similarly to the quasi-static case, the trajectories can sometimes be optimized locally for lower Δv.

6. MANIFOLD METHOD

6.1. Manifold generation

Given a closed orbit, one is interested in the behavior of trajectories that are close to this original orbit. The differential of the Poincaré map encodes this information [8]. It has 5 non-trivial eigenvalues λ_i, see figure 3. Except for neutral/stable Halos, the eigenvalues follow this pattern

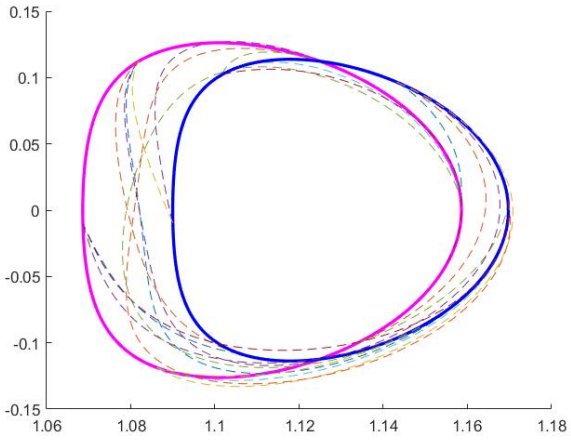

Fig. 7. A sampling of Lambert arc for two Halo orbits

- $\lambda = 1$, the continuation direction for closed Halo
- $|\lambda| < 1$, the stable direction
- $|\lambda| > 1$, the unstable direction
- $\lambda = e^{\pm i\theta}$, a pair of complex eigenvalues of norm 1

If the unstable direction is excited, the trajectory will diverge from the original trajectory by a factor of λ each orbit. The deviation ϵ after N is related to the original deviation ϵ_0 orbit by $\epsilon \sim \lambda^N \epsilon_0$. It follows that in the CR3BP, it is possible to insert into a unstable trajectory with an arbitrary small nonzero maneuver. Analogously, if a perturbation ϵ_0 is applied in the stable direction then the perturbations will be damped by a factor of λ each orbit i.e. $\epsilon \sim \lambda^N \epsilon_0$ hence converging to the original orbit. When orbits are propagated backward in time, their behavior are inverted; stable orbits diverge and unstable orbits converge to the original trajectory. The collection of all unstable/stable trajectories generated from a given orbit is called the unstable/stable manifold of the orbit. A method to generate all unstable trajectories is the following (for $\lambda > 0$): pick an initial perturbation ϵ_0 and a number of branches to be generated N, then the kth perturbation is given by

$$\epsilon_k = \lambda^{k/N} \epsilon_0 \tag{23}$$

for $k \in \{0, \cdots, N-1\}$, when $k = N$, the trajectory obtained is the same as $k = 0$ but with an effective shift in the time variable. If $\lambda < 0$, the kth perturbation is given by

$$\epsilon_k = [\lambda^2]^{k/N} \epsilon_0 \tag{24}$$

Given w_u, the unstable direction, there still remains the choice of whether to apply perturbations in the direction of $+w_u$ or $-w_u$, this choice is only relevant in the case $\lambda > 0$. In the case of $\lambda < 0$ equation 24 covers all trajectories. In the former case, the trajectories that go away from the Moon

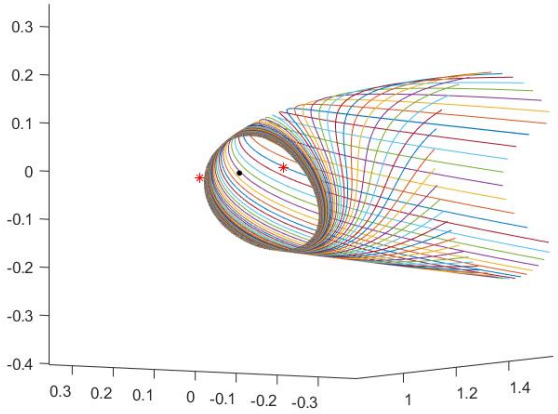

Fig. 8. Exterior unstable trajectories of the orbit with V_z = 268.5 m/s, A_z = 65 294.6 km

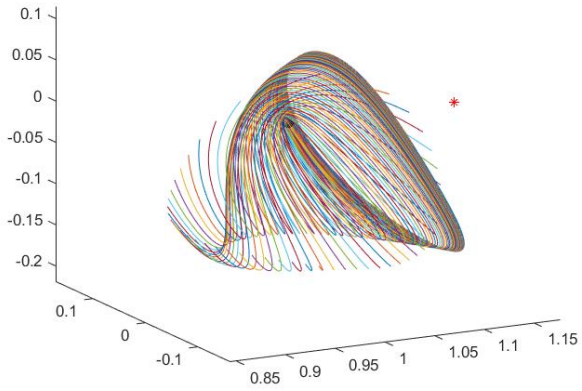

Fig. 9. Interior unstable trajectories of the orbit with V_z = 268.5 m/s, A_z = 65 294.6 km

form the exterior manifold, the ones that go towards the Moon form the interior manifold. Examples of such trajectories are shown in figure 8 and 9. The same procedure can be applied to the stable manifold with backward time propagation. The manifolds are two dimensional objects for which one possible parametrization is α and t, with $\epsilon = \alpha\epsilon_0$ and t the propagation time.

$$(\vec{r}_u, \vec{v}_u) \leftrightarrow (\alpha_u, t_u) \tag{25}$$
$$(\vec{r}_s, \vec{v}_s) \leftrightarrow (\alpha_s, t_s) \tag{26}$$

with $t_u > 0$ and $t_s < 0$

6.2. Manifold Intersection

This section will be devoted to finding intersections between the unstable manifold of a departure Halo orbit A and the stable manifold of a target Halo orbit B. To begin, it is noteworthy to point the problem in a mathematical framework.

Find a set of 4 parameters α_u, α_u, t_u, t_s such that

$$\vec{r}_u = \vec{r}_s \tag{27}$$

There are 3 equations to solve, the x,y,z components of equation 27, but 4 variables. It is expected that if there is an intersection at all, there is a whole 1 dimensional subspace, analogously to how 2 planes intersect in a line. To compute the intersection, several manifold branches are generated, typically on the order of ~ 100. The integration time is chosen such that the trajectory are propagated far enough from the initial orbit to make sure the two manifolds intersect. Next a spline interpolation is done on the trajectory with respect to t to obtain a uniform grid in time with a resolution on the order of hours. A triangulation of the manifold must then be done, firstly by triangulating the variables α and t as in figure 10 and then forming the triangles in 3-D space as in figure 11.

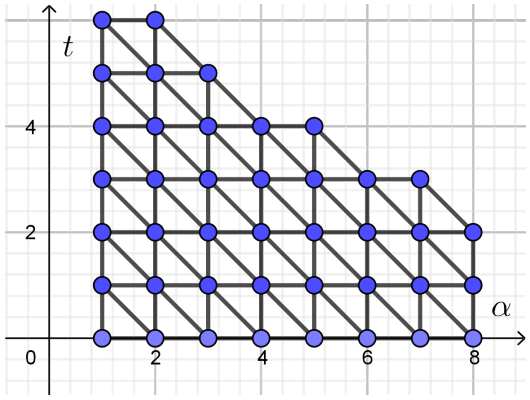

Fig. 10. Example of the triangulation of a grid

Once the two manifolds are triangulated, a Möller triangle-triangle intersection algorithm is performed [10] to obtain a set of intersections, as shown in figure 12. The intersections being found, one must reconstruct the variables $\alpha_u, t_u, \alpha_s, t_s$, that produced these intersections. A simple linear approximation based on the triangle vertices can be employed. Given that the following 3 vertices are known, with intersection point r^*

$$(\alpha_1, t_1) \leftrightarrow r_1 \tag{28}$$
$$(\alpha_2, t_2) \leftrightarrow r_2 \tag{29}$$
$$(\alpha_3, t_3) \leftrightarrow r_3 \tag{30}$$

The following linear approximation can be made

$$r = C_0 + C_\alpha \alpha + C_t t \tag{31}$$

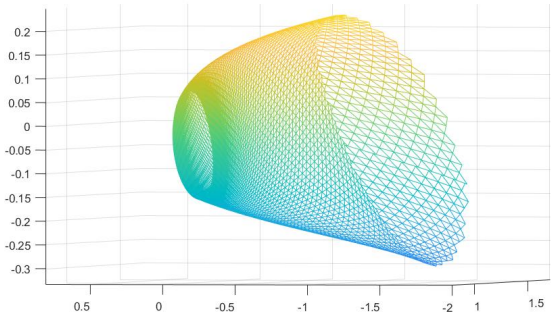

Fig. 11. Triangulation of an exterior unstable manifold

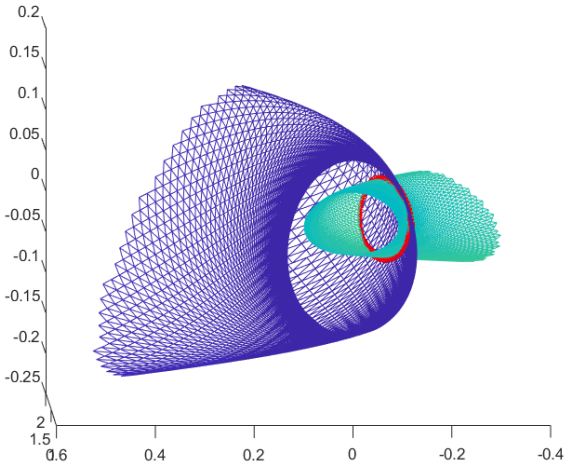

Fig. 12. Intersection of exterior manifolds starting at V_z = 75 m/s, A_z = 18 023 km to the end halo at V_z = 225 m/s, A_z = 55445 km

With constants C_0, C_α, C_t chosen to satisfy relation 28, 29 and 30. By simple resolution of the system (algorithmically done with a least square) one can obtain α^* and t^* that has $r = r^*$. From this, velocities v^* can also be obtained. As the surface is triangulated more and more finely, this approximation gets more accurate. In the case that higher accuracy is needed, a refinement procedure can be performed. As a result, a list of intersections is obtained, the one with lowest Δv is chosen.

6.3. Energy consideration

A constant of motion of the CR3PB is the Jacobi constant.

$$J = \frac{1}{2}v^2 - \frac{\mu_E}{|\vec{r} - \vec{r}_E|} - \frac{\mu_M}{|\vec{r} - \vec{r}_M|} - \frac{1}{2}(\vec{\omega} \times \vec{r})^2 \qquad (32)$$

For the L_2 family the Jacobi constant has the behavior described in figure 13. It is interesting to note that the energy of the orbit reaches a plateau and then decreases. This fact will be used in case 11,12,13 and 14 of next section.

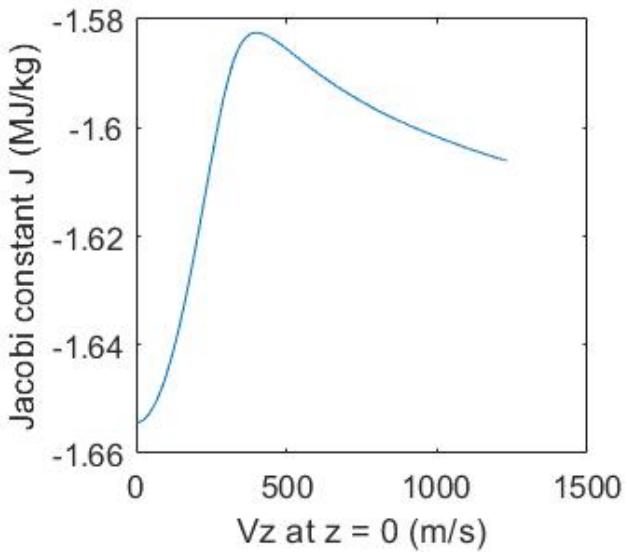

Fig. 13. Jacobi constants for the L2 Southern Halo orbit

7. RESULTS

7.1. Study cases

The study cases considered in this article are trying to cover qualitatively different orbit transfers. The cases considered are

1. Close Halo to Halo, $V_z = 42 \rightarrow 83\ m/s$
2. Close Halo to Halo, $V_z = 232.5 \rightarrow 285\ m/s$
3. Far Halo to Halo, $V_z = 42 \rightarrow 285\ m/s$
4. Opposite direction from #3
5. Close NRHO to NRHO, $V_z = 549 \rightarrow 634.5\ m/s$
6. Close NRHO to LOP-G, $V_z = 792.5 \rightarrow 884.5\ m/s$
7. Far NRHO to LOP-G, $V_z = 549 \rightarrow 884.5\ m/s$
8. Oppositive direction from #7
9. Neutral Halo to LOP-G, $V_z = 423.5 \rightarrow 884.5\ m/s$
10. Opposite direction from #9
11. Halo to NRHO, same jacobi, $V_z = 315.5 \rightarrow 586.5\ m/s$
12. Opposite direction #11
13. Halo to LOP-G, same jacobi, $V_z = 274.5 \rightarrow 883\ m/s$
14. Opposite direction of #13

Table 3. Methods comparison

Case	V_z (m/s)		$A_z(A)$ or $P_e(P)$ (10^3 km)		Quasi-static (m/s)	Manifold (m/s)	Lambert (m/s)	ToF (hours)	Comments
	Dep.	Arr.	Dep.	Arr.					
1	42	83	10.04A	19.98A	48.92	49.76	48.55	125.03	Close Regular Halo
2	232.5	285	57.24A	68.50A	72.13	69.32	72.56	128.82	Close Regular Halo
3	42	285	10.04A	68.50A	331.02	312.28	340.72	119.6	Far Regular Halo
4	285	42	68.50A	10.04A	331.02	312.44	356.64	138.8	Backward of 4
5	549	634.5	7.03P	4.71P	17.09	18.42	17.05	121.84	Close NRHO
6	792.5	884.5	2.32P	1.49P	11.44	12.33	11.48	91.74	Close NRHO
7	549	884.5	7.03P	1.49P	53.41	61.87	54	105.18	Far NRHO
8	884.5	549	1.49P	7.03P	53.41	59.1	52.84	111.55	Backward of 7
9	423.5	884.5	13.64P	1.49P	79.15	N/A	83.39	134.71	Neutral Halo to NRHO
10	884.5	423.5	1.49P	13.64P	79.15	N/A	81.51	130.63	Backward of 9
11	315.5	586.5	72.21A	5.88P	80.3	33.75	44.98	340.16	Same Jacobi constant
12	586.5	315.5	5.88P	72.21A	80.3	33.78	54.89	293.56	Backward of 11
13	274.5	883	66.5A	1.51P	173.05	81.71	110.11	281.95	Same Jacobi constant
14	883	274.5	1.51P	66.5A	173.05	80.3	146.2	209.11	Backward of 13

7.2. Analysis

The comparison between the methods are shown in table 3. The quasi-static and manifold methods are limiting cases for an infinite time of flight. For the manifold method, a finite time of flight is possible by jumping in and out of the manifold arcs. The faster one wants to achieve the transfer, the more Δv will be paid, eventually defeating the purpose of the manifold transfer. For Lambert arcs, the time of flight is well defined and is given in the column ToF.

One fact is immediately clear: if the orbits are close then the 3 methods give essentially the same results within less than 10%. There is at least two ways the manifold method could be improved. The first is to consider very large flight time, this is because the manifolds eventually re-intersect very far away from the original orbit. This was discarded due to the flight time being too large. The other way would be to consider much higher resolution of the manifold, both in α and in t in the hope of bringing back very fine structure of the manifold which was lost during the discretization procedure. Other than such a resolution making the intersection computation prohibitive, these solutions would be more sensitive to maneuver errors.

Where the manifold method starts to be of interest is for far Halo orbits, even though the saving is only in the order of 10%, the difference in absolute Δv starts to be significant. Interestingly for far NRHO to NRHO, the manifold method does not give any improvement as compared to the Lambert arc. That could be due to the geometrically complicated shape of the manifolds for NRHO which may require much higher resolution than what was considered in this article.

The instance where the manifold method is clearly superior is when the transfer is done between two orbits of the same Jacobi constant. There, savings from 25% to 45% as compared to Lambert arcs are observed. This translates to a saving in Δv that varies between 10 m/s and 65 m/s.

7.3. Conclusion

A benchmark for the cost Δv between any two L_2 southern Halo orbits was established with the quasi-static method (fig 5). Two other methods were compared for the transfer cost Δv between orbits: Optimized Lambert arcs and manifold intersections. The three methods results are essentially identical for orbits that are close, but differs for far orbits. The case of interest occurs when the transfer is between two orbits of same energy where substantial savings is obtained. The case of far NRHO to NRHO interestingly enough is made worse with the manifold method, higher resolution or longer transfer time may help in finding better transfers. It is concluded that the only instance where the manifold method substantially saves Δv is when the transfers are done between orbits of similar energy.

One important improvement to consider would be to increase the degree of freedoms of the transfers; this article only considered pure unstable/stable manifolds which have two degree of freedoms per manifold (4 in total). By also exciting the central eigenspace i.e. $|\lambda| = 1$, one can increase the search space and possibly reducing the cost Δv. The main drawback would be the doubling of the search space for intersections. Not being pure a unstable/stable manifold, they would also require at least three, potentially large, burns to

perform the transfer.

Another important aspect to consider is the robustness of these solutions in an ephemeris dynamics. On one hand the notion of manifold is destroyed for ephemeris models but new dynamics of the Earth-Moon-Sun system can now be exploited.

8. REFERENCES

[1] "Lunar outpost sustaining human space exploration by utilizing in-situ resources with a focus on propellant production," International Astronautical Congress 2018, IAC-18,A5,1,5,x46282.

[2] S. Lizy-Destrez, "Rendezvous optimization with an inhabited space station at EML2," 25th International Symposium on Space Flight Dynamics, ISSFD, 2015.

[3] G. Gómez, A. Jorba, J. Masdemont, and C. Simó, "Study of the transfer from the earth to a halo orbit around the equilibrium pointl1," *Celestial Mechanics and Dynamical Astronomy*, vol. 56, no. 4, pp. 541–562, Aug 1993.

[4] G. Gómez et al, "Connecting orbits and invariant manifolds in the spatial restricted three-body problem," Caltech, 2004.

[5] V. Szebehely, "Theory of orbits. the restricted problem of three bodies," Academic Press, New York, 1967.

[6] NASA, "General mission analysis tool (GMAT)," 2016.

[7] S. K. Wang et al., "Dynamical systems, the three-body problem and space mission design," Caltech, 2000.

[8] Norman R. Lebovitz, "Ordinary differential equations, chapter 9 stability ii: maps and periodic orbits," http://people.cs.uchicago.edu/ lebovitz/odes.html.

[9] D. Torre Sangra, E. Fantino, "Review of lambert's problem," 25th International Symposium on Space Flight Dynamics ISSFD, 2015.

[10] T. Moeller, "A fast triangle-triangle intersection test," Stanford University, 1992.